

SUSCEPTIBILITY MAPPING OF LANDSLIDES IN CHAMPLAIN CLAY FROM A DIGITAL LANDSLIDE INVENTORY

Pete Quinn

GeoEngineering Centre, Queen's University, Kingston, Ontario, Canada, quinn@geoladm.geol.queensu.ca

D. Jean Hutchinson, Mark S. Diederichs, R. Kerry Rowe, Jackie Alvarez

GeoEngineering Centre, Queen's University, Kingston, Ontario, Canada

RÉSUMÉ

Une base de données détaillée de larges glissements de terrain dans l'est du Canada est en développement via l'analyse de photos aériennes. L'incidence et absence de glissements de terrain dans une sous-section de la région étudiée ont été comparées statistiquement avec les paramètres du terrain, incluant la géologie de surface, l'épaisseur du mort-terrain (ou profondeur au roc), élévation au dessus du niveau de la mer, les caractéristiques des cours d'eau au voisinage des glissements de terrain. L'analyse est utilisée pour développer une méthodologie pour la cartographie de la susceptibilité aux glissements de terrain à partir d'observations statistiques. La cartographie de la susceptibilité supportera le développement de cartes d'aléas de glissements de terrains, qui seront utilisées pour gérer le risque aux infrastructures linéaires.

ABSTRACT

A comprehensive digital database of large landslides in sensitive clay in eastern Canada is being compiled through aerial photo analysis. The incidence and absence of landslides in a selected subset of the study area has been compared statistically with specific terrain attributes, including surficial geology, thickness of overburden soils, elevation above sea level, and characteristics of the associated watercourse. This analysis is used to develop a methodology for landslide susceptibility mapping based on observed statistical trends. The susceptibility mapping will support the development of landslide hazard maps, to be used in assessment and management of landslide risk to linear infrastructure.

1 INTRODUCTION

This paper describes ongoing efforts to develop a digital inventory of landslides in sensitive clay in eastern Canada, and then presents a preliminary landslide susceptibility map, prepared at the regional scale. The purpose of this work is to identify areas of high or low relative landslide susceptibility, which will serve to focus more detailed studies of specific areas along linear infrastructure corridors. This work does not attempt to define individual hazards at a local scale, but rather to prioritize hazard areas within a much larger study area.

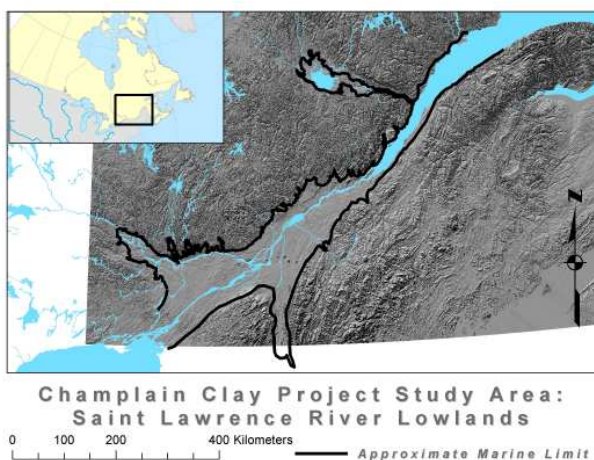


Figure 1. Project study area.

Figure 1 illustrates the extent of the study area, which includes the lowlands of eastern Ontario and southern Quebec, which were subject to deposition of marine sediments (i.e. Champlain clay) in the post-glacial Champlain Sea subsequent to the withdrawal of the Wisconsin ice sheet roughly 10,000 years ago. The study area is bounded to the north by the Precambrian rocks of the Grenville Province of the Canadian Shield, and to the south by folded sedimentary rocks of the Appalachian Orogen. The marine sediments, which range up to nearly 200m in thickness, are generally underlain by sedimentary rocks of the Saint Lawrence Platform and the Appalachian Orogen.

The marine silts and clays deposited in salt water have been modified due to the processes of isostatic rebound and erosion, and subsequent leaching with fresh water. This has resulted in much of the finer sediments becoming sensitive, which means that their remoulded strength is much lower than their undisturbed strength. These soils suffer from a particular geological hazard, namely retrogressive earth flows, which tend to occur suddenly and without warning, typically involving very gentle terrain, and often affecting very large areas, occasionally up to several square kilometres.

Retrogressive landslides in sensitive clay pose a hazard to the population of south-eastern Quebec, and in particular to built infrastructure such as roads, railways, pipelines, power transmission lines and other linear infrastructure. This paper uses a new digital inventory of landslides in sensitive clay in eastern Canada to help model landslide susceptibility. The paper then illustrates

how this interpretation might be used to assess hazards, at the regional scale, along linear infrastructure corridors.

2 A DIGITAL INVENTORY OF LANDSLIDES IN CHAMPLAIN CLAY

2.1 Development Process

The development of a digital inventory of landslides in sensitive clay has been described by Quinn *et al.* (2007a). The first major step involved compilation and digitization of landslide data from the literature. These data represent a snapshot of the distribution of landslides across the study area, but a biased one, since the literature generally describes only notable landslides, with few exceptions.

A very small fraction of the total landslide inventory is represented in the literature, which also includes two paper-based inventories: one for the area around Ottawa (Fransham and Gadd, 1977), and one for the Province of Québec (Chagnon, 1968). The Ottawa inventory appears to be very detailed and complete, but only covers the western end of the study area, and is not available in digital form. The Quebec inventory includes only a limited number of illustrations of known landslides in Quebec. There are therefore significant gaps in publicly available landslide inventory data. It was therefore necessary to study digital terrain models and aerial photographs to construct a more complete inventory.

The Quebec government is actively working on landslide hazard mapping at large scale for selected communities. This work was initiated in the 1980s following the procedure outlined by Lebuis *et al.* (1982), and continues today following the procedure outlined by Gouvernement du Québec (2005). The primary difference between that work and the present research is the scale of study; this work examines landslide distribution and susceptibility at the regional scale, rather than local scale, for the purpose of prioritizing further detailed study at selected areas within the larger study area.

An initial reconnaissance-level inventory was completed using various interpretive scenes (e.g. hillshade, slope angle) from available digital elevation models covering the study area (Canadian Digital Elevation Data, 2000 and Shuttle Radar Topography Mission, 2000). This reconnaissance survey revealed a large number of potential large landslide features; however, smaller features (i.e. width less than about 150 m) or more subtle features (i.e. less pronounced scarp) were often missed, leading to an underestimate of landslide incidence.

Aerial photos (National Air Photo Library, 1994) were then used to compile a more detailed inventory of possible landslide features in a representative section of the study area – NTS 31H (Figure 2). The inventory work was completed at medium scale (1:50,000) for two reasons: this scale of photography is widely available for the entire study area; and, the study area is too large to work with large scale photos, which are only available for selected areas, and not at consistent scales. Use of 1:50,000

scale photos limits the inventory to features with a minimum width of about 50-80 m (varies with photo quality), which therefore excludes many small features, but generally captures most of the more important retrogressive landslides.

2.2 Preliminary Results

The landslide database includes a total of 2649 possible landslide features in NTS 31H. These features have been subdivided into the following categories:

- 1 – probable retrogressive landslide;
- 2A – arcuate scarp; possible abandoned river meander, more likely retrogressive landslide;
- 2B - arcuate scarp; possible retrogressive landslide, more likely abandoned river meander;
- 3 – subtle indication of possible retrogressive landslide;
- 4 – arcuate scarp associated with episodic minor landslide and/or erosion activity; and
- 5 – arcuate scarp along the Saint Lawrence River, possibly associated with large retrogressive landslide, or alternatively a river erosion feature.

For the purposes of analysis, types 1, 2A and 3 have been grouped as probable retrogressive landslides. This sub-group includes a total of 1264 features (~ 48% of all possible landslide features). The remaining features are more likely, on average, to not be retrogressive landslides, and some may not be landslides at all, since it is not always possible to distinguish certain river erosion features (e.g. abandoned meanders) from the scarps of old landslides when working at 1:50,000 scale. For present purposes, Type 5 features have not been included with the probable retrogressive landslides. This likely excludes a number of very large retrogressive landslides; however, further study is required to properly distinguish these large features along the Saint Lawrence River.

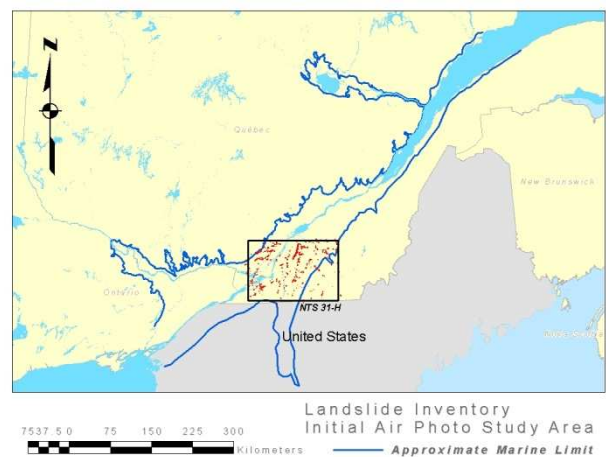


Figure 2. Aerial photo inventory area – NTS 31H.

Figures 2 and 3 illustrate the extent of the aerial photo survey (i.e. NTS 31H) and the general distribution of probable landslide features throughout the area. Figure 4

presents a larger scale view of part of NTS 31H to illustrate the typical distribution of landslide features along the middle reach of the Yamaska River, which has a high

spatial density of landslides. Probable retrogressive landslides are shown in red and other features shown in black in Figure 3.

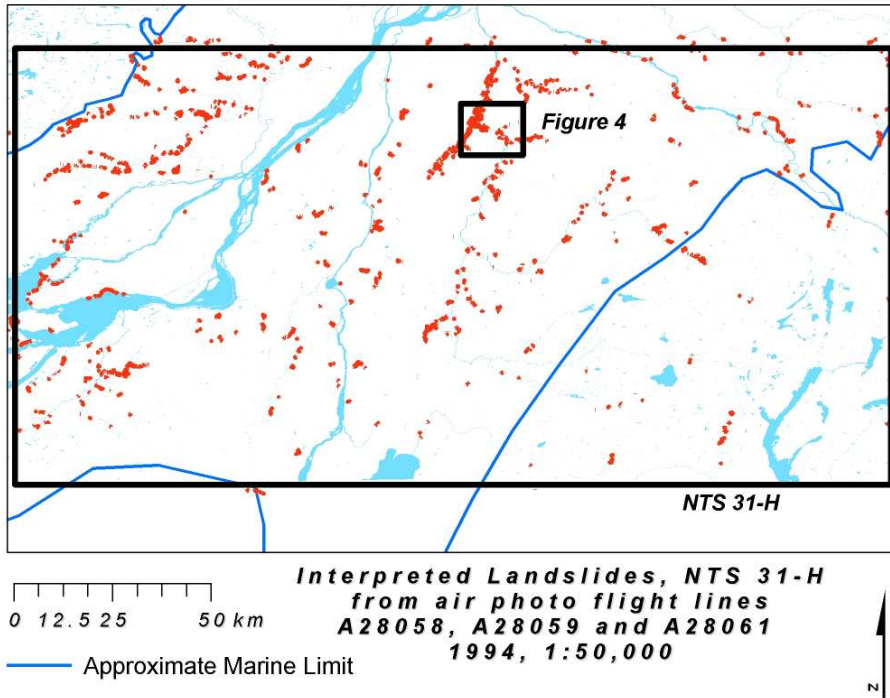


Figure 3. General distribution of all observed landslide features within NTS 31H.

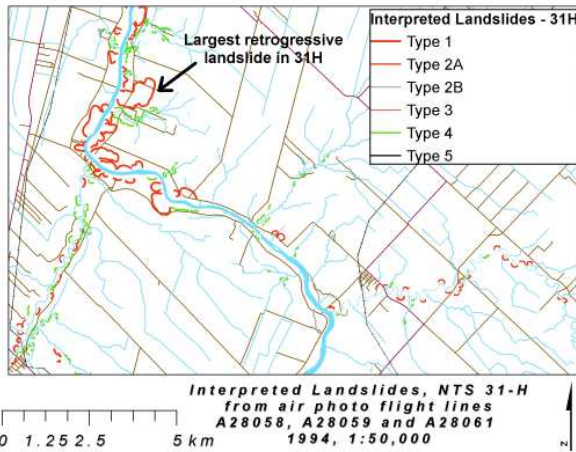


Figure 4. Detailed view of landslide distribution along a section of the Yamaska River.

2.3 Statistical Characteristics of the Inventory

Plots of size (surface area) versus frequency for all interpreted landslide features and for probable retrogressive landslides are presented in Figure 5.

The most common size of landslide feature is on the order of about 2-3,000 m² for all landslide features, and roughly 4-6,000 m² for the retrogressive landslides. If we project the trend lines to cross the horizontal axis, it appears that

the largest single landslide in this part of the study area would be expected to be on the order of 2×10^6 m², or roughly 200 ha. This is approximately one order of magnitude larger than the Saint-Jean-Vianney landslide of 1971 that killed 31 people, and the same order of magnitude as the Saint-Alban slide of 1894 (Wilson and Mackay, 1919). The largest retrogressive landslide observed in NTS 31H, as represented by the green triangle in Figure 5, is shown on Figure 4 along the Yamaska River.

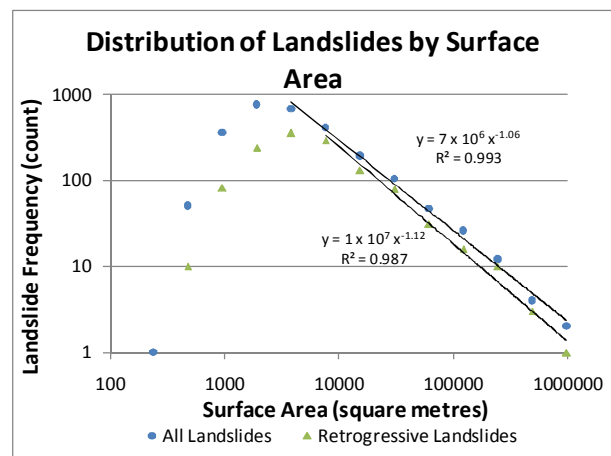


Figure 5. Frequency distribution of landslide size by surface area.

Figure 6 shows the distribution of orientation of the openings of landslide craters. It can be seen that there are four dominant modes: zero (or 360), 120, 180-195, and 270-285 degrees. These four modes reflect the most common orientations of landslide features. Since most landslides open in the direction of an adjacent watercourse (e.g. as illustrated in Figure 4), it follows that these modes are perpendicular to the most common directions of the associated streams affected by landslides. This suggests that landslides tend to be more common along watercourses that run east-west and north-south (approximately). Note that there are strong relationships between drainage characteristics and the structure of the underlying bedrock; however, a discussion of this factor is outside the scope of the present paper.

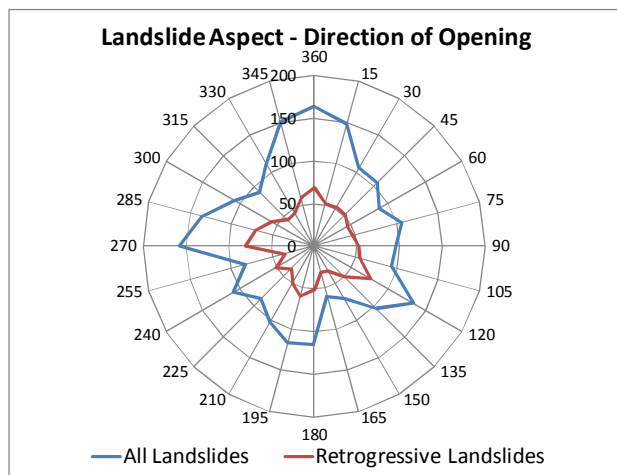


Figure 6. Frequency distribution of orientation of the landslide openings.

Landslides in the study area are expected to occur, generally, in the marine silts and clays deposited in deep, calm water and subsequently altered by uplift, erosion and leaching. Figure 7 shows the frequency distribution of soil types associated with landslides in comparison with the total area represented by each soil type within NTS 31H. The most common soil types, which are interpreted from Natural Resources Canada (1994) are till (moraine), marine deposits (which includes marine silt, clay and sand) and alluvial deposits. Landslides are under-represented, on a per unit area basis, in the till deposits (both moraine and veneer), absent in bog deposits, and significantly over-represented in the marine deposits. There is therefore a clear, anticipated relationship between soil type and landslide incidence at the scale of available geological mapping (1:1,000,000).

It has been suggested (e.g. Rankka *et al.* 2004, Lefebvre, 1996) that there are relationships between the thickness of overburden soils (or more precisely, the depth to underlying bedrock) and the incidence of landslides in sensitive clay. Figure 8 presents the frequency distribution of landslides in relation to the thickness of overburden soil, in an effort to explore this possibility. Soil thickness data were interpreted at the location of each

landslide feature from Natural Resources Canada (2004) and Couture and Gauvreau (2006).

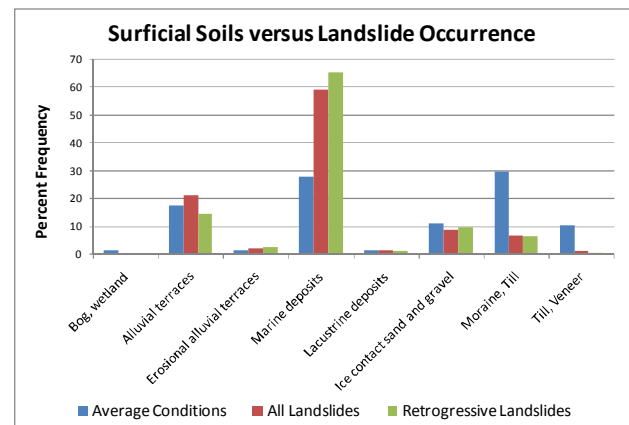


Figure 7. Frequency distribution of landslides by surficial soil type.

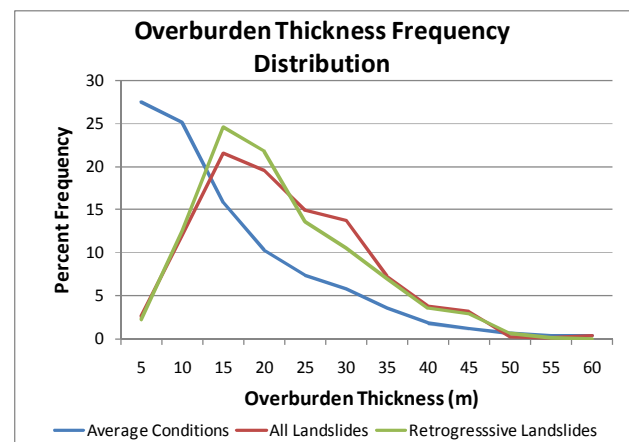


Figure 8. Frequency distribution of landslides by thickness of overburden soils.

It is evident that landslide features are more common at intermediate overburden thickness, and are absent or under-represented at very small or large thicknesses, when compared with the average distribution of thickness throughout the study area. Note that overburden thickness varies from zero to 168 m throughout the study area, but landslides are most common where overburden ranges between about 10 to 40 m.

Rankka *et al.* (2004) have also suggested a relationship between ground elevation and incidence of landslides in sensitive clay. This possibility has been explored by obtaining the elevation of the scarp for each landslide feature and comparing the landslide elevations to elevations throughout the study area, where elevation above sea level is interpreted from Canadian Digital Elevation Data, Level 1 (2000). As shown in Figure 9, there are at least three elevation ranges where landslide features tend to be more common, out of proportion with the average elevation conditions: 20, 30 and 40 m above sea level. By contrast, landslides are under-represented, when compared with average conditions, at most other

elevations. One might postulate that the dominant elevation modes are associated with specific geological conditions, associated with different stages of deposition. In fact there are extensive alluvial terraces east of Montreal at typical elevations of about 35 m (Natural Resources Canada, 1994). This may be an explanation for the pronounced decrease in landslide incidence between 30 and 40 m in Figure 9.

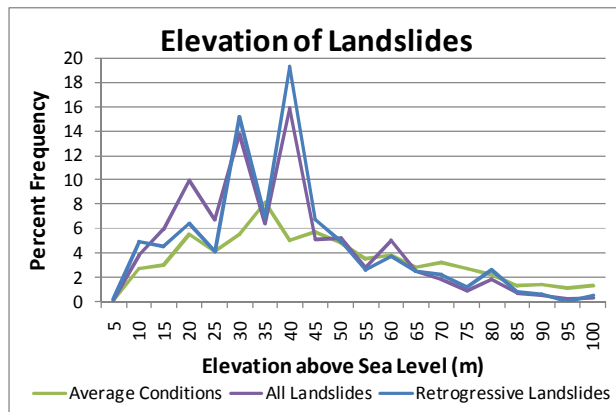


Figure 9. Frequency distribution of landslides by ground elevation above sea level.

A preliminary review of aerial photos for selected locations within the overall Champlain clay study area by Quinn *et al.* (2007b) suggests that there are relationships between the nature of drainage features and the incidence or absence of landslides. In particular, landslides tend to be associated with river of intermediate width or flow and with deep channels. Lefebvre (1996) suggests that retrogressive landslides tend to be more common along rivers of intermediate age, and are less common along young and fully established drainages. Bjerrum *et al.* (1969) suggest that the occurrence of landslides along rivers through sensitive clay areas can be related to the gradient and flow in relation to a stable condition for a river with similar characteristics. It has therefore been decided to explore characteristics of the drainage systems and attempt to relate them to the occurrence of landslides in the study area.

The first characteristic that has been explored is stream order, which is expected to correlate with streamflow volume. Figure 10 illustrates what is meant by stream order. First order streams are the youngest streams at the outer reaches of the drainage system. Where two first order streams merge, the resulting stream is second order. The Yamaska River, which is known to have a high density of large landslides and is the largest feature in Figure 10, is eighth order along much of its length. Note that fourth, fifth and seventh order streams are absent from this small part of the study area, but are present elsewhere. The Saint Lawrence River is a ninth order stream. Note that this interpretation is generated within GIS based on an interpreted stream network obtained from a digital elevation model (from Canadian Digital Elevation Data, Level 1, 2000). This interpreted stream network is very similar to the actual stream

network, with some minor differences, particularly for the lower order streams.

Figure 11 illustrates the relationship between interpreted stream order and interpreted flow accumulation, which is also generated within the GIS. The flow accumulation values represent the total surface area that is calculated to direct its overland flow to any given point on the map. This value may differ from actual flow, depending on differences in runoff and infiltration, which could vary with soil type, vegetative cover or other factors. The relationship, which is plotted in log-log space, shows a linear trend, however with considerable scatter and overlap in calculated flow between adjacent order values. Nevertheless, there is clearly a trend for typical flow to increase with increasing value of stream order.

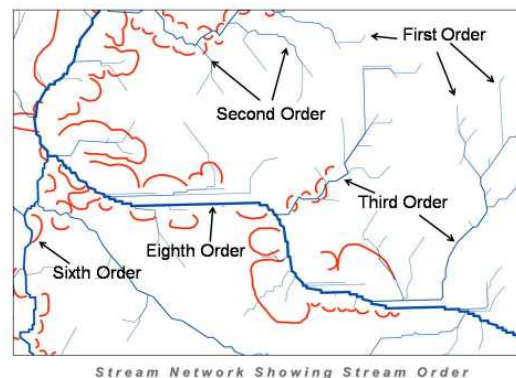


Figure 10. Interpreted stream network showing stream order.

Streamflow data were obtained from Ministère du Développement durable, de l'Environnement et des Parcs (2007) for 21 permanent streamflow monitoring stations, and compared with GIS-calculated flow accumulation. There is a very strong correlation between observed mean annual flow and calculated flow accumulation, as illustrated in Figure 12. These results suggest that interpreted flow accumulation may be used as an estimate for mean annual flow with confidence, and that interpreted stream order is a reasonable surrogate for streamflow.

The order of the nearest adjacent stream has been obtained for each landslide feature, and the results are summarized in Figure 13. To do this, a buffer was first created along each drainage feature of third or higher order, extending 500 m to either side. Next, the number of landslides was determined within all buffers for each stream order. Finally, the number of landslides within the stream order buffers was divided by the total surface area to obtain a density of landslides per unit area for each order. It is readily observed in Figure 13 that landslide density is high for streams with order 5 to 8, low for order 4, and very low for streams of order 3 and 9. Landslide density is also very low outside the stream buffers, which includes all lands not located within 500 m of a third (or higher) order stream. These findings tend to agree with Lefebvre (1996) who suggested retrogressive landslides

are more common along intermediate drainages, and less common along young (less developed) or older (fully developed) watercourses.

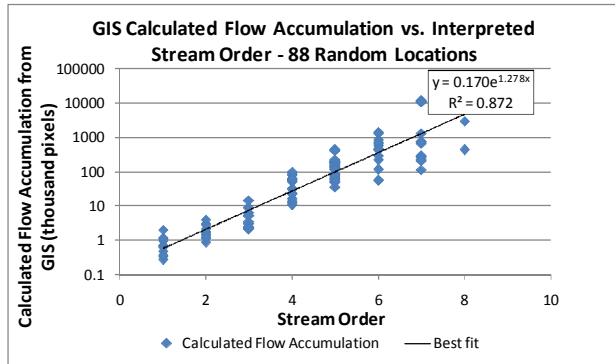


Figure 11. Relationship between calculated flow accumulation and interpreted stream order.

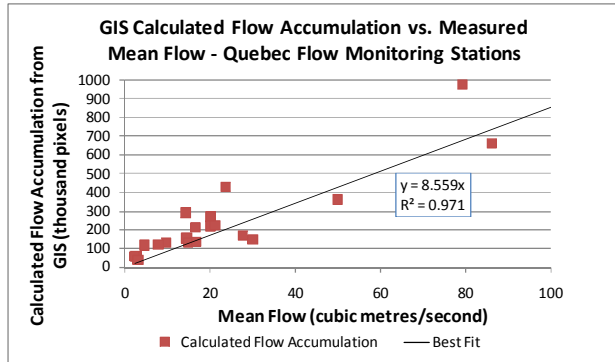


Figure 12. Relationship between calculated flow accumulation and observed annual average streamflow.

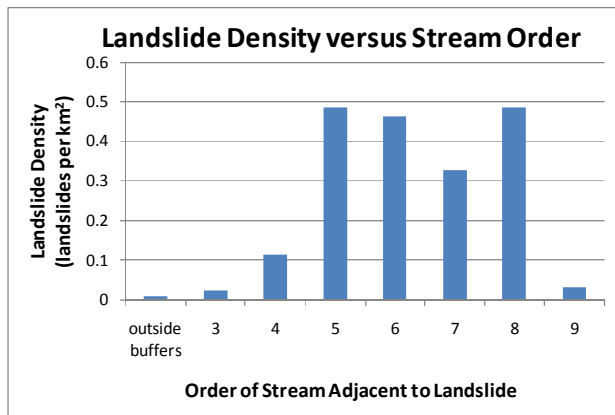


Figure 13. Landslide density versus interpreted stream order.

3 LANDSLIDE SUSCEPTIBILITY MAPPING

3.1 Development Process

A simple multi-variate procedure has been devised to obtain a preliminary assessment of landslide susceptibility throughout the air photo survey area (NTS 31H). Four variables have been considered: surficial soil type;

thickness of overburden soils; elevation above sea level; and, order of the nearest adjacent stream (within 500 m). A unitless, dimensionless, relative susceptibility value, S_{LS} , was obtained through raster algebra in the GIS using the following formula:

$$S_{LS} = X_{SO}(X_{ST} + X_{OB} + X_E) \quad (1)$$

Where

- S_{LS} = relative landslide susceptibility
- X_{SO} = stream order coefficient
- X_{ST} = surficial soil type coefficient
- X_{OB} = overburden thickness coefficient
- X_E = ground elevation coefficient

Each of the coefficients is calculated by dividing the incidence of landslides (i.e. frequency or density) by the incidence of average conditions. For example, in the case of marine deposits, 59% of all landslides occur in this soil type, which represents about 28% of the total surface area. X_{ST} is therefore calculated as $59/28 = 2.1$ for this soil type. Similarly, $X_E = 1.38$ for ground elevation equal to 15 m ($22/16$). Equation (1) yields values ranging from 0.003 to 6.8, where a higher number represents higher relative landslide susceptibility.

3.2 Preliminary Results

The outcome of the preliminary landslide susceptibility mapping is illustrated in Figure 14. High susceptibility is represented by red tones, and low is represented by green. The black dots represent the locations of mapped landslide features. It can be seen that the majority of the landslide features are captured within higher susceptibility areas - approximately 80% of retrogressive landslides occur where the calculated susceptibility value is 2 or greater. It is also noted, however, that there are many areas of high interpreted susceptibility where landslides are absent. Further analysis using other aspects of the drainage system may reduce this conservatism.

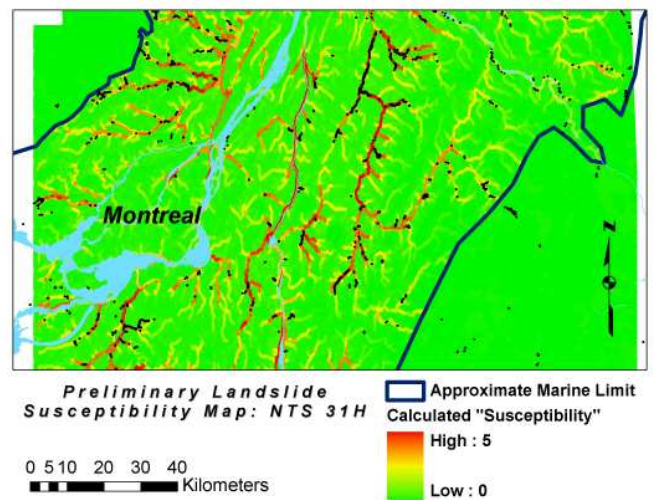


Figure 14. Preliminary landslide susceptibility map.

3.3 Analysis

It is possible to test the validity of the susceptibility model by comparing the landslide density to calculated susceptibility value, as illustrated in Figure 15. The incidence of landslides increases with susceptibility value, as expected. In the case of retrogressive landslides, there is a sharp increase at $S_{LS} = 2.0$. The increase is somewhat more gradual in the case of the larger inventory of all landslides, which includes smaller landslides and some probable non-landslide features.

Given the results illustrated in Figure 15, it might be prudent to use $S_{LS} = 2.0$ as distinguishing between relatively low and high susceptibility. One might further note that such susceptibility values (i.e. $S_{LS} > 2.0$) represent a very small proportion of the total study area, and that lower values (notable $S_{LS} = 1.0$, which comprises roughly 80% of the study area) are much more dominant. Thus, selection of $S_{LS} = 2.0$ as a discriminating criteria to distinguish between low and high susceptibility eliminates over 80% of the study area from consideration, and thus serves to narrow the focus to a much smaller area with much higher probable landslide susceptibility.

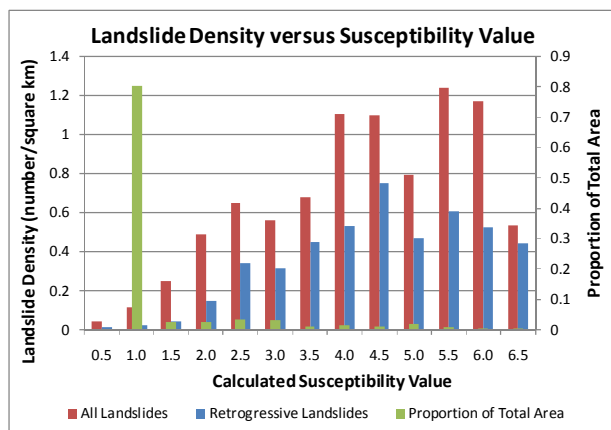


Figure 15. Landslide density versus calculated susceptibility value.

3.4 Application to Linear Infrastructure

One can explore the use of this sort of susceptibility map by considering a set of two hypothetical linear rights of way, with one on either side of the Saint Lawrence River, as located in Figure 16. Note that while this is conceptually similar to the locations of the CN and CP Rail lines or Quebec highways 20 and 40, the lines in this Figure were drawn arbitrarily, and do not coincide spatially with actual linear infrastructure. They could similarly represent power transmission lines or pipelines, and were chosen for illustrative purposes only.

If we create a buffer (arbitrarily 500 m either side of the rights of way) along both features, we can examine landslide susceptibility along the length of the railways and ignore the remainder of the study area, thus focussing attention along the rights of way. Figure 16 shows landslide susceptibility along the full length of both

features. Figure 17 is a larger scale view of one section with a particularly high frequency of landslide-susceptible areas. Note that in this case, red is for $S_{LS} > 2.0$, and green is for $S_{LS} < 2.0$, or more simply, red equals “high” relative susceptibility and green implies “low” susceptibility. In Figure 17, there are eight zones of high susceptibility along a length of approximately 20 km. This could serve to focus more detailed efforts to understand site-specific landslide hazards at those eight specific locations.

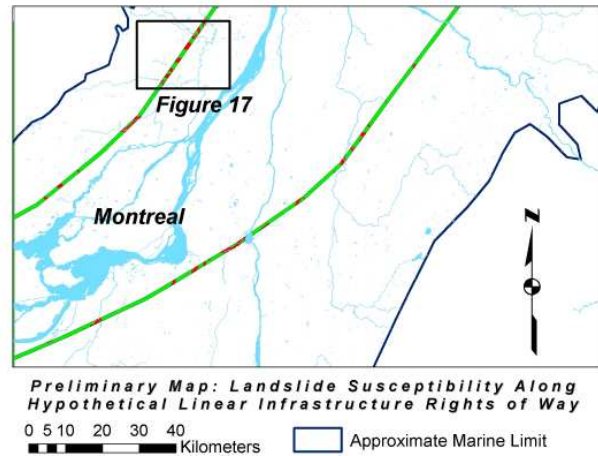


Figure 16. Landslide susceptibility along hypothetical linear infrastructure corridors.

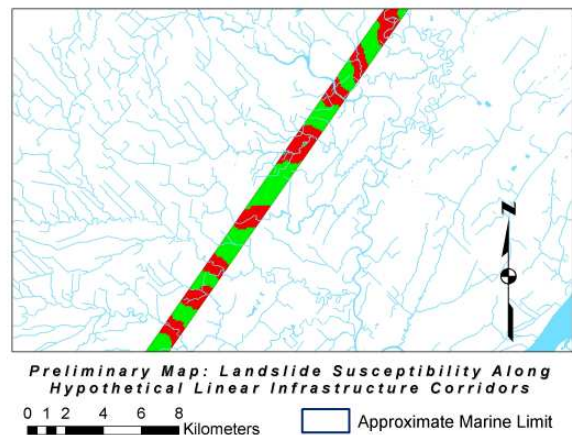


Figure 17. Landslide susceptibility along a hypothetical linear infrastructure corridor – example section with high density of landslide susceptible areas.

3.5 CONCLUSIONS AND FURTHER WORK

The early results of this work are encouraging, and show that it is possible to identify areas of relatively high and low landslide susceptibility within the GIS, on a regional scale, on the basis of readily available geospatial information.

The first area of focus for further development will be to explore additional characteristics of the interpreted drainage systems, such as stream gradient, streamflow and channel geometry (specifically, channel width and

depth, bank slopes, and channel curvature). Consideration of these additional characteristics within the GIS analysis is expected to allow refinement of the susceptibility model and yield better predictions of landslide occurrence and absence within the inventory area.

The next area of focus will be to test the model outside NTS 31H, in other parts of the Champlain clay study area. The model will be refined on the basis of that analysis, and then extended to cover the whole study area. Such a complete susceptibility model would then support the development of landslide hazard maps at the regional scale. Note, however, that hazard maps require consideration of temporal distribution of landslide events, which is not considered in the spatial modelling leading to the susceptibility maps in this paper. Such hazard maps will then support the development of risk models and risk maps at the regional scale, which will serve the purpose of focussing attention to high hazard and risk areas along, for example, linear infrastructure corridors.

ACKNOWLEDGEMENTS

This work was supported financially by the GEOIDE network, and NSERC NCE, and the Railway Ground Hazards Research Program, funded by NSERC CRD, Transport Canada, CN Rail and CP Rail. Student funding through the NSERC PGS program is gratefully acknowledged. The work benefited substantially from the leadership and interest of Mario Ruel at CN Rail. The writers are grateful to Marten Geertsema of the BC Forest Service and Réjean Couture of NRCAN for their constructive review comments. Réjean Couture also provided valuable advice on quality assurance during development of the landslide inventory from aerial photo interpretation.

REFERENCES

- Bjerrum, L., Loken T., Heiberg S. and Foster, R. 1969. A field study of factors responsible for quick clay slides. *Proceedings of the 7th International Conference on Soil Mechanics and Foundation Engineering*, 531-540.
- Canadian Digital Elevation Data. Level 1 [Digital Elevation Model]. 2000. Natural Resources Canada, Sherbrooke, Quebec, Canada. Available www.geobase.ca. [Accessed September 2006 to April 2007].
- Chagnon, J.-Y. 1968. Les coulées d'argile dans la province de Québec. *Naturaliste Canadien*, 95: 1327-1343.
- Couture R. and Gauvreau D. 2006. Development of a 3-D geological model as a tool towards natural hazards mitigation, St. Lawrence River Valley, Eastern Canada. GSC Contribution #2005439. In *10th IAEG Congress: Engineering geology for tomorrow's cities*, Nottingham, United Kingdom, 6-10 September 2006
- Fransham, P.B., and Gadd, N.R. 1977. Geological and geomorphological controls of landslides in Ottawa Valley, Ontario. *Canadian Geotechnical Journal*, 14: 531-539.
- Gouvernement du Québec. 2005. Cartographie des zones exposées aux glissements de terrain dans les dépôts meubles – Guide d'utilisation des cartes de zones de contraintes et d'application du cadre normative. ISBN 2-550-42506-5.
- Lebuis, J., Robert, J.-M., and Rissmann, P. 1982. Regional mapping of landslide hazard in Quebec. In *Symposium on Slopes on Soft Clays*, Swedish Geotechnical Institute Report No. 17, Linköping, 205-262.
- Lefebvre, G. 1996. Soft Sensitive Soils. *Chapter 24 In: Landslides, Investigation and Mitigation*, Special Report 247, Transportation Research Board, National Research Council, National Agency Press, Washington, DC, 607-619.
- Ministère du Développement durable, de l'Environnement et des Parcs. 2007. *Suivi hydrologique de différentes stations hydrométriques* [Hydrological data]. Available <http://www.cehq.gouv.qc.ca/suivihydro/> (Accessed 19 October 2007).
- National Air Photo Library. 1994. *A28058, photos 2 to 34, 49 to 83, 86 to 122, 141 to 172, 175 to 205, 213 to 245, 248 to 278; A28059, photos 1 to 6, 21 to 57, 60 to 97, 113 to 147, 150 to 186, 198 to 234, 237 to 275; A28061, photos 1 to 13, 21 to 57* [aerial photographs]. 1:50,000. Ottawa, Ontario: Department of Energy, Mines and Resources.
- Natural Resources Canada. 1994. *Surficial Materials of Canada, Map 1880a*, Geological Survey of Canada, Terrain Sciences Division. Available <http://gsc.nrcan.gc.ca/urbgeo/> [Accessed September 2006].
- Natural Resources Canada. 2004. *Urban Geology of the National Capital Area – Drift Thickness*, Geological Survey of Canada, Terrain Sciences Division. Available <http://gsc.nrcan.gc.ca/urbgeo/> [Accessed September 2006].
- Quinn, P.E., Hutchinson, D.J. Diederichs, M.S., Rowe, R.K., Harrap, R., Alvarez, J. 2007a. A Digital Inventory Of Landslides In Champlain Clay, *Canadian Geotechnical Conference*, Ottawa, Ontario.
- Quinn, P.E., Hutchinson, D.J. and Rowe, R.K. 2007b. Toward a risk management framework: sensitive clay landslide hazards affecting linear infrastructure in eastern Canada, *1st North American Landslide Conference*, Vail, Colorado.
- Rankka, K., Andersson-Skold, Y., Hultén, C., Larsson, R., Leroux, V. and Dahlin, T. 2004. Quick clay in Sweden. *Report 65*, Swedish Geotechnical Institute.
- Shuttle Radar Topography Mission. [Digital Elevation Model]. 2000. United States Geological Survey. Available <http://gsc.nrcan.gc.ca/urbgeo/> [Accessed September 2006].
- Wilson, M.E. and MacKay, B.R. 1919, Landslide adjacent to Rivière Blanche, St. Thuribe, Parish of St. Casimir, Portneuf County, P.Q., In: *Report on Mining Operations in the Province of Quebec during 1918, Quebec Bureau of Mining Annual Report 1918*, 152-156.